Mariam K. Glob [1]
Saleem A. Hussain [2]
Khalidah H. Al-Mayalee [1]

[1] *Department of Physics, College of Education for Girls, University of Kufa, AL-Najaf, IRAQ*
[2] *Department of Physics, College of Education, University of Al-Qadisiyah, Al-Diwaniyah, IRAQ*

Preparation and Characterization of Titanium Dioxide Nanoparticles by Laser Ablation in Liquid

In this study, titanium dioxide (TiO_2) nanoparticles were created by pulsed laser ablation in a liquid media. One hundred, two hundred, or three hundred pulses were fired from a Q-switched Nd:YAG laser, each packing 480 mJ of energy. The results demonstrated the efficient production of pure TiO_2 nanoparticles crystalline in the brookite form. The filed-emission scanning electron microscopy (FE-SEM) scans disclosed spherical particles measuring between 50.81 and 71.22 nanometers in diameter. The Brunauer-Emmett-Teller (BET) study showed that the surface area of TiO_2 was quite high, ranging from 82.44 to 98.67 m^2/g. Oxygen (O) and titanium (Ti) peaks that stood out during the EDX examination confirmed that the nanoparticles were pure. Furthermore, FTIR identified a unique absorption peak at 657 cm^{-1}, which is indicative of stretching vibrations of Ti-O-Ti. This study was effective in developing a method for producing well-characterized TiO_2 nanoparticles with potential applications across a wide range of industries.

***Keywords*:** Titanium dioxide; Nanostructures; Laser ablation; Nd:YAG laser
Received: 17 October; **Revised:** 19 November; **Accepted:** 26 November 2023

1. Introduction

Materials with dimensions ranging from one to one hundred nanometers, or nanometer dimensions, is one method to define nanomaterials. The distinctive and innovative characteristics of these materials distinguish them as cutting-edge technologies employed across diverse domains. An advantageous characteristic of nanomaterials in comparison to conventional materials is their improved thermal, mechanical, chemical, and electrical properties. In addition to their superior resistance to erosion and corrosion, nanomaterials may also be more lightweight and durable than conventional materials [1]. Electrical and thermal conductivity are also exceptionally high. Nanomaterials are utilized in significant fields such as materials research, health, energy, electronics, and the environment. In the electronic industry, nanomaterials are employed in the fabrication of flexible electronics, high-resolution displays, and compact electronics. In the medical field, nanomaterials are employed in the fabrication of specialized drugs and minuscule medical apparatus [2]. Titanium dioxide (TiO_2) was selected as the material for our research due to its distinctive attributes, which encompass excellent efficiency, affordability, chemical inertness, non-toxicity, photocatalytic activity, photo stability, and the ability to degrade a wide variety of organic molecules [3]. TiO_2 possesses an exceptionally high refractive index, second only to diamonds, which enables the development of novel applications, including imparting whiteness and opacity to plastics, paper, fibers, food, and cosmetics [4]. Rutile and anatase comprise the tetragonal phase of TiO_2 crystallization, while brookite comprises the orthorhombic phase.

The aim of this study is to develop a laser liquid ablation technique employing titanium dioxide and deionized water (DIW) to create nanomaterials with novel characteristics. X-ray diffraction (XRD), Brunauer-Emmett-Teller (BET), field-emission scanning electron microscopy (FE-SEM), energy-dispersive x-ray spectroscopy (EDX) and Fourier-transform infrared (FTIR) spectroscopy were used to characterize the acquired samples.

2. Experimental Part

The laser ablation approach was chosen as a means of synthesizing nanoparticles due to its perceived simplicity and cost-effectiveness. The procedure entailed immersing high-purity TiO_2 in a solution of distilled water (DDDW) at ambient temperature. Initially, a mass of 5 g of TiO_2 was subjected to compression within a mold of 2 cm in diameter for a duration of 15 min., without the inclusion of any additional substances. Subsequently, the TiO_2 was carefully positioned at the base of a quartz container, which was then filled with a volume of 4 mL of liquid. The subjects were exposed to a Q-switched Nd:YAG laser, which emitted light at a wavelength of 1064 nm. The laser had a pulse duration of 7 ns and operated at a repetition frequency of 5 Hz. The laser energy employed for the TiO_2 material was 480 mJ per pulse.

Subsequently, the crushed TiO_2 underwent laser bombardment using 100, 200, and 300 pulses. The

laser beam is focused onto the nanostructure, inducing high-energy interactions at the surface. The term "plasmon" was introduced at this phase. Plasmon's, which refer to electromagnetic oscillations arising from the modulation of electron density, are produced through the interaction between a laser and a metal surface. The presence of plasmon impurities exerts an influence on chemical reactions and enhances the diffusion of titanium dioxide atoms. The laser beam was directed towards the TiO_2 target by use of a focusing lens possessing a focal length of 100 mm.

3. Results and Discussion

The XRD patterns of the synthesized TiO_2 nanoparticles samples are illustrated in Fig. (1). The peaks in the XRD patterns have confirmed the presence of nanomaterials exhibiting significant crystallinity. The brookite TiO_2 phase is indicative of the TiO_2 nanoparticles that were synthesized in this investigation (JCPDS card no. 29-1360). A distinct domain (120) peak at approximately $2\theta=25.33°$ is observed in the diffraction patterns of the prepared samples. This peak is attributed to a rhombohedral structure of the TiO_2 phase, characterized by brookite lattice constants $a=b=c$ 0.37852 nm and angles $\alpha=\beta=\gamma\leq90°$. Additionally, the absence of peaks corresponding to other substances in the XRD patterns indicates that the samples were manufactured with an exceptionally high level of purity.

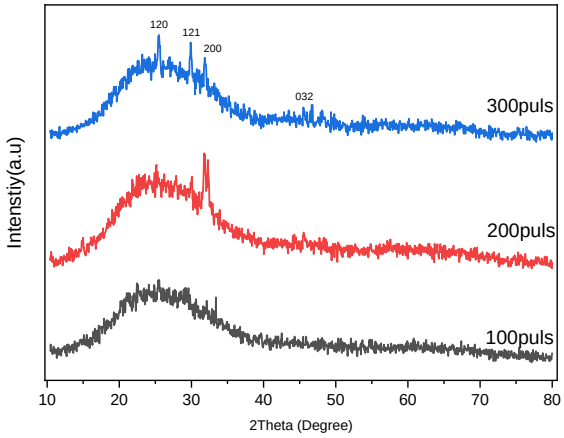

Fig. (1) XRD patterns of the TiO_2 nanoparticles by laser ablation method

The XRD results of TiO_2 nanopowders synthesized in this work are summarized in table (1). The Debye-Scherrer equation [5] was employed to ascertain the average crystalline size of TiO_2 nanoparticles through the broadening of the brookite TiO_2 peaks at various 2θ in the model. Table (2) shows the findings indicated that the prepared samples exhibited an average crystal size ranging from 3.30 to 2.31 nm.

Table (1) XRD results for the prepared TiO_2 nanoparticle by laser ablation method

Laser pulses	2θ Standard	2θ Observed	d-Spacing (Å) standard	d-Spacing (Å)	(hkl)
100	25.339	25.54	3.5120	3.5167	120
	30.807	29.544	2.7290	2.6270	121
	32.790	34.794	2.7290	2.4053	200
	46.071	45.949	1.9685	2.0122	032
200	25.339	25.144	3.5120	3.5167	120
	30.807	29.894	2.7290	2.6285	121
	32.790	31.894	2.7290	2.8208	200
	46.071	45.994	1.9685	2.9654	032
30z	25.339	25.44	3.5120	3.51021	120
	30.807	29.944	2.7290	2.6774	121
	32.790	31.994	2.7290	2.5149	200
	46.071	45.444	1.9685	2.0432	032

Table (2) Average crystallite sizes of the prepared TiO_2 nanoparticles synthesized by laser ablation method

Laser pulses	Average crystallite size (D) (nm)
100	3.30
200	3.03
300	2.31

Figures (2-4) illustrates the findings of the isotherms of nitrogen (N_2) adsorption and desorption of TiO_2 nanoparticles synthesized by pulsed laser ablation at 100, 200 and 300 pulses. Hysteresis loops will form between the adsorption and desorption curves due to the irregular distribution of pore sizes in the ready nanoparticles. Utilizing an inert gas, nitrogen gas in this instance, was intended to eliminate any absorbent molecules from the substance. Hysteresis loops that exist between the adsorption and desorption curves are crucial and foundational for elucidating certain nanostructure-related details of the prepared samples.

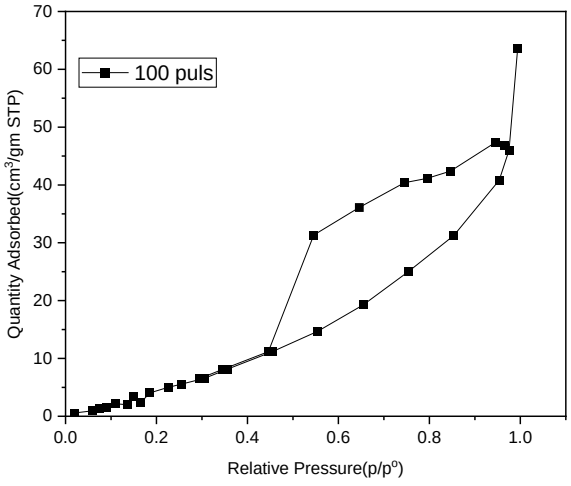

Fig. (2) N_2 adsorption-desorption of TiO_2 nanoparticles synthesized at 100 pulses

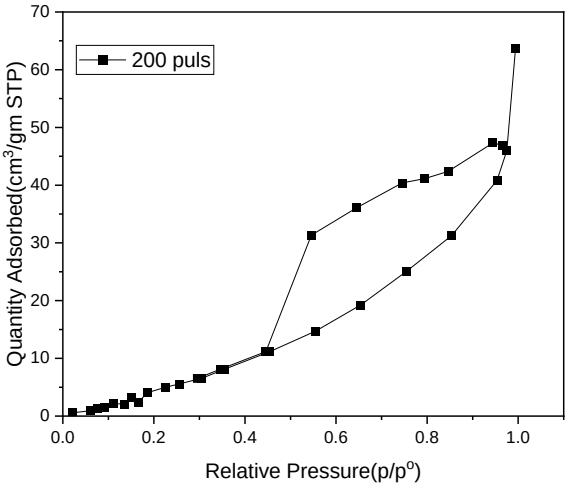

Fig. (3) N_2 adsorption-desorption of TiO_2 nanoparticles synthesized at 200 pulses

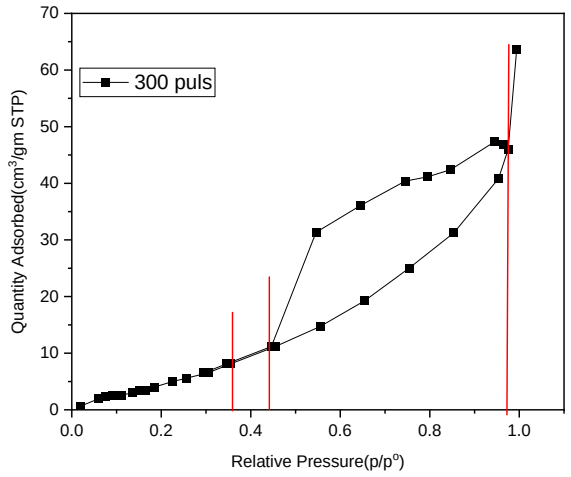

Fig. (4) N_2 adsorption-desorption of TiO_2 nanoparticles synthesized at 300 pulses

The existence of the previously mentioned hysteresis loop provides an accurate depiction of the apertures within the nanomaterial, as evidenced by the loop's dimensions and area. The linear isotherm plot illustrates the variation in the quantity adsorbed in relation to p/p_0. The presence of a porous material is indicated by the synthesized samples' isotherms, which display a progressive change in the adsorption-desorption branch over a significant pressure range (p/p_0). The sample preparation processes involved 100, 200, and 300 pulses, as is evident. A linear depiction of the isotherm exhibits the presence of four distinct regions. As illustrated in Fig. (4), the area can be categorized into four distinct regions. The regions delineated in the figure are as follows: the isotherm reveals a progressive increase in adsorption in the first region, where the relative pressure (p/p_0) is less than 0.37; this indicates that the samples contain microspores. Within the second region, the relative pressure ranges from 0.37 to 0.46, and the presence of faint hysteresis loops on the isotherm suggests the presence of mesopores in the samples [6]. Within the third region, characterized by relative pressures ranging from 0.45 to 0.96, the isotherm exhibits a discernible concentration of capillaries. This expression suggests that the hysterical loop in this particular region is notably different in both breadth and distinction when compared to other regions. This characteristic suggests the existence of distinct capillary concentrations. Furthermore, it illustrates the correlation between the adsorbate present in the ambient phase and the adsorbate that is on the surface of the adsorbent under constant temperature and equilibrium conditions [7]. In the fourth region, where the relative pressure is greatest (0.96), a minor hysteresis loop is discernible, suggesting the presence of more sizable mesopores [8]. According to the data in the table, the specific surface area of TiO_2 nanoparticles produced by laser ablation for samples with 100, 200, and 300 pulses was approximately 82.44, 86.43, and 96.67 m^2/g, respectively. The evaluation of the pore size distribution pattern was conducted using the Barret-Joyner-Halenda (BJH) method on the desorption branch of the N_2 isotherm [9], as illustrated in figures (5) and (6). The findings indicate that the samples synthesized by the laser ablation method (100, 200, 300 pulses) have, on average, pore sizes of 3.52, 3.57, and 5.28 nm, and pore volumes of 0.044, 0.047, and 0.048 cm^3/g, respectively.

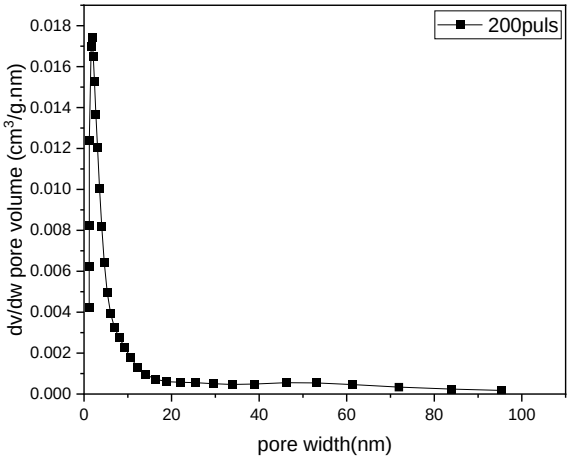

Fig. (5) Pore size distribution of TiO_2 synthesized by laser ablation method at 200 pulses

The examination of the surface morphology of the prepared samples was conducted utilizing FE-SEM, as illustrated in figures (7-9). These figures display FE-SEM images of the samples 100, 200, and 300 pulses. The particles depicted are of spherical and irregular shapes, exhibiting consistent distributions. These particles may be single particles or clusters of particles, with average diameters of 50.81, 62.33, and 73.22 nm for the aforementioned samples (100, 200, and 300 pulses), as indicated in table (4).

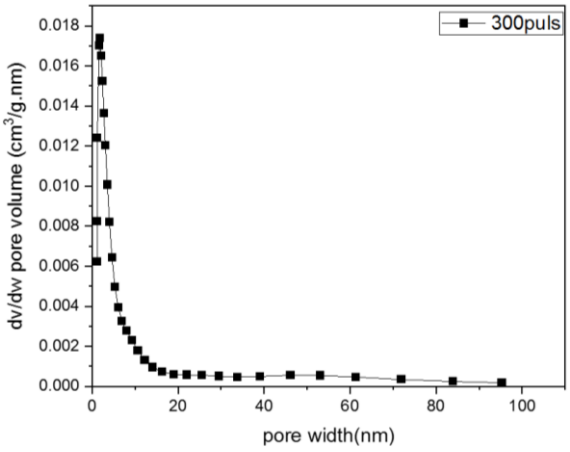

Fig. (6) Pore size distribution of TiO_2 synthesized by laser ablation method at 300 pulses

Table (3) Surface area, average pore diameter and volume of TiO_2 nanoparticles samples prepared at 100, 200, 300 pulses by laser ablation method

Laser pulses	Surface area (m^2/g)	Average pore diameter (nm)	Total pore volume (m^3/g)
100	82.44	3.52	0.044
200	86.43	3.57	0.047
300	98.67	5.28	0.048

Table (4) Average lengths, diameters, and aspect ratio of TiO_2 samples prepared at 100, 200 and 300 pulses by laser ablation method

Laser pulses	Average length (nm)	Aver diameter (nm)	Aspect ratio (length/diameter)
100	520	85	3.22
200	1200	97	6.94
300	1800	110	9.32

The EDX spectra of TiO_2 nanoparticles synthesized via laser ablation at 100, 200, and 300 pulses are illustrated in figures (10-12). The EDX analyses confirmed that the produced samples had the specified atomic composition. The findings demonstrate that the spectra comprised intense peaks for titanium (Ti) and oxygen (O), which provide confirmation that the synthesis of pure TiO_2 nanoparticles was effective.

The FTIR spectrum obtained from the laser ablation-prepared TiO_2 nanoparticles is depicted in Fig. (13) and is summarized in table (5). The broad absorption band observed between 3300 and 3800 cm^{-1} can be attributed to the stretching vibration of the hydroxyl O-H group at 3500 cm^{-1}. This vibration is caused by the physical absorption of water and serves as an indication that moisture is present in the samples [10,11]. The faint bands at 2060 and 1630 cm^{-1} are attributed to water in solution that has been chemically absorbed by O-H bending groups. The peak at 657 cm^{-1} was attributed to Ti-O-Ti stretching vibrations, which indicated that titanium dioxide absorbed a significant amount of energy as a result of Ti-O bridge stretching or bending vibration rather than Ti-O stretching [12].

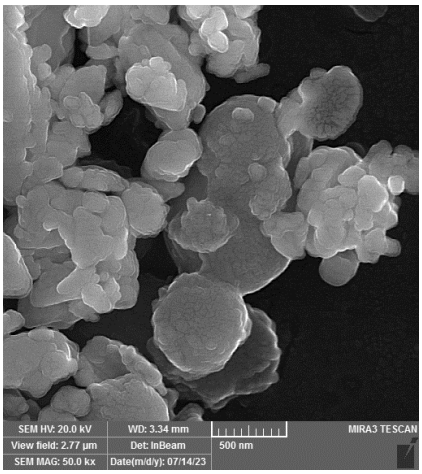

Fig. (7) FE-SEM image of TiO_2 nanoparticles prepared by laser ablation method at 100 pulses

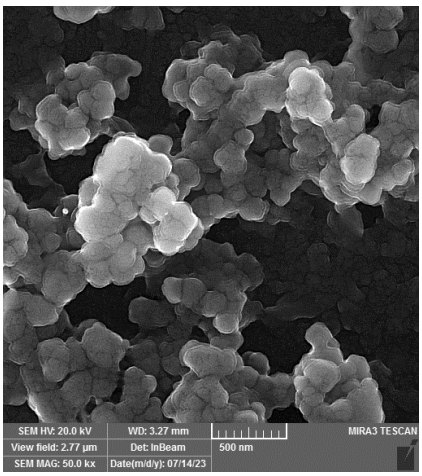

Fig. (8) FE-SEM image of TiO_2 nanoparticles prepared by laser ablation method at 200 pulses

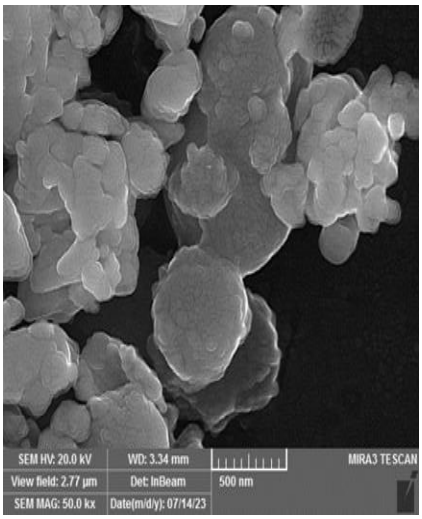

Fig. (9) FE-SEM image of TiO_2 nanoparticles prepared by laser ablation method at 300 pulses

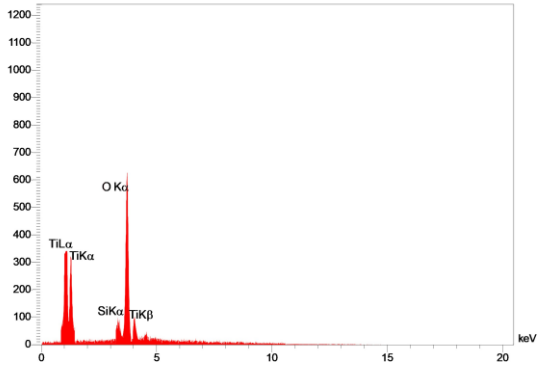

Fig. (10) EDX spectrum of TiO_2 nanoparticles by laser ablation at 100 pulses

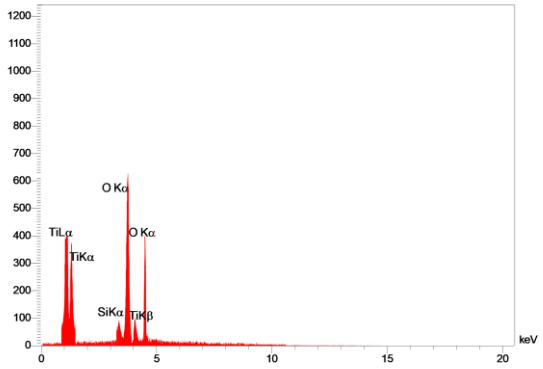

Fig. (11) EDX spectrum of TiO_2 nanoparticles by laser ablation at 200 pulses

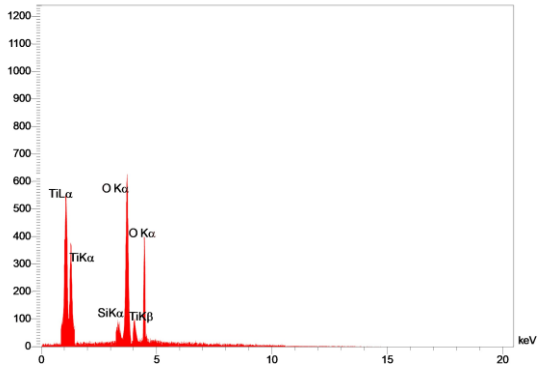

Fig. (12) EDX spectrum of TiO_2 nanoparticles by laser ablation at 300 pulses

The vibrational modes of R-TiO_2 at the Δ point can be mathematically represented in the following irreducible ways: The expression

$\Delta opt = A1g + A2g + A2u + 2B1u + B1g + B2g + E_g + 3E_u$

denotes the following configurations: Δopt signifies Raman active mode, Δu signifies infrared active mode, and E signifies degenerate mode. The bands associated with Ti-O and Ti-O-Ti vibrations undergo a shift with respect to δ.

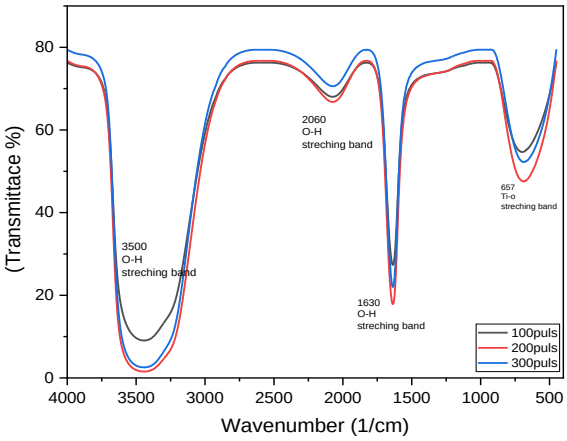

Fig. (13) FTIR spectra of TiO_2 nanoparticles prepared by laser ablation at 100, 200 and 300 pulses

Table (5) Assignments of FTIR bonds of the prepared TiO_2 prepared by laser ablation

Assignments	Wavenumbers (cm^{-1})
O – H stretching	3500
O – H stretching	2060
O – H bending	1630
Ti-O-Ti stretching	657

4. Conclusion

The empirical evidence suggests that the utilization of the pulsed laser bombardment method is a feasible strategy for producing titanium dioxide particles. The experimental methodology employed in this study entailed the utilization of titanium dioxide powder as the primary material, which was subjected to bombardment by a pulsed laser. The TiO_2 nanoparticles displayed a brookite phase, which was distinguished by a notably elevated level of crystallinity. The synthesized TiO_2 samples exhibit an average size distribution ranging from 50.81 to 71.22 nm. The surface area was ranging from 82.44 m^2/g to 98.67 m^2/g for the samples of TiO_2. The existence of absorption peak at a wavenumber of 657 cm^{-1} was confirmed.

References

[1] N. Baig, I. Kammakakam and W. Falath, "Nanomaterials: A review of synthesis methods, properties, recent progress, and challenges", *Mater. Adv.*, 2(6) (2021) 1821-1871.

[2] N. Kumar, N. Maiti and S. Thomas, "Insights into Plasmon-Induced Dimerization of Rhodanine–A Surface-Enhanced Raman Scattering Study", *J. Phys. Chem. A*, 127(20) (2023) 4429-4439.

[3] S. Zhang et al., "Advanced titanium dioxide-polytetrafluorethylene (TiO_2) nanocomposite coatings on stainless steel surfaces with antibacterial and anti-corrosion properties", *Appl. Surf. Sci.*, 490 (2019) 231-241.

[4] H.A. Al-kaisy and L. Al-Gebory, "Preparation and Characterization of TiO_2-ZrO_2 Coating Prepared by Sol-Gel Spin Method", *Iraqi J. Mech. Mater. Eng.*, 20(3) (2020) 257-267.

[5] C. Wolf, **"Physical Properties of Semiconductors"**, Prentice Hall (NyY, 1989).
[6] G.M.A. AI-Rumahi, "Fabrication and Characterization of TiO_2 Dye sensitized Solar Cells", PhD dissertation, University of Kufa.
[7] C. Erkey and M. Türk (eds.), "Chapter 6 - Thermodynamics and kinetics of adsorption of metal complexes on surfaces from supercritical solutions", Supercritical Fluid Science and Technology, Elsevier, 8 (2021) 73-127.
[8] K.L.A. Cao et al., "Sustainable porous hollow carbon spheres with high specific surface area derived from Kraft lignin", *Adv. Powder Technol.*, 32(6) (2021) 2064-2073.
[9] A.M. Negrescu et al., "Metal Oxide Nanoparticles: Review of Synthesis, Characterization and Biological Effects", *J. Func. Biomater.*, 13(4) (2022) 274.
[10] S.L. Brantley and N.P. Mellott, "Surface area and porosity of primary silicate minerals", *Amer. Mineral.*, 85(11/12) (2000) 1767-1783.
[11] S.A.R. Hasan, J.A.S. Salman and S.S. Al-Jubori, "Characterization of Titanium dioxide (TiO_2) Nanoparticles Biosynthesized using Leuconostoc spp. Isolated from Cow's Raw Milk: Characterization of (TiO_2) Nanoparticles", *Proc. Pakistan Acad. Sci.: B. Life Enviro. Sci.*, 60(1) (2023) 133-142.
[12] M. Fathy and H. Hamad, "Influence of calcination temperatures on the formation of anatase TiO_2 nano rods with a polyol-mediated solvothermal method", *RSC Adv.*, 6(9) (2016) 7310-7316.

